Int J Anal Bio-Sci Vol. 13, No 2 (2025)

<Research Article>

Development of a phenylpyruvate-specific dehydrogenase through structure-based enzyme designs and its application in a phenylpyruvate assay

Momoka Nakamura[1] and Yoshiaki Nishiya[1,2,*]

Summary A phenylpyruvate (PPY)-specific dehydrogenase was developed through the structure-based enzyme design of *Geobacillus stearothermophilus* lactate dehydrogenase (gs-LDH). Docking analysis of gs-LDH revealed that PPY binding at the active site was energetically stabilized by three mutations. Among these, the Q102A and A239G mutants were found to improve PPY specificity, and the double mutant showed an additive effect. However, the pyruvate (PYR) dehydrogenase activity of the double mutant remained at approximately 70% of that of wild-type gs-LDH (WT). Subsequently, the T249A mutation, which spatially expanded around the catalytic residue, was introduced into the double mutant. The PPY/PYR specific activity ratio of the triple mutant was 4100% compared to 42% of the WT; thus, a PPY-specific enzyme was successfully developed. *In silico* analysis showed that the distance between the catalytic residue and PYR in the triple mutant was approximately 2.3 Å farther than that in WT, suggesting a decrease in the proton transfer efficiency. A PPY endpoint assay reagent containing the triple mutant was prepared, and its practicality was preliminarily confirmed.

Key words: Phenylpyruvate, Lactate dehydrogenase, *Geobacillus*, Tertiary structure, Mutagenesis

1. Introduction

Various enzymes have been used to analyze biological samples. Despite their functional and structural similarities, lactate dehydrogenase (LDH) and malate dehydrogenase (MDH) differ in substrate specificity[1]. By analyzing the crystal structures of the diagnostic enzyme *Geobacillus stearothermophilus* MDH under various conditions, we succeeded in determining four tertiary structures corresponding to each step in the catalytic reaction cycle [enzyme alone (apo-enzyme), enzyme+coenzyme, enzyme+coenzyme+substrate (open form), and enzyme+coenzyme+substrate (closed form)][2]. A comparison of these structures elucidated the detailed mechanism of the structural changes leading to the enzyme reaction in the closed form[2-5]. These findings explain the high substrate specificity of MDH. Furthermore, structural and molecular dynamics analyses provided an understanding of the differences in substrate specificity between MDH and LDH[4].

The results highlighted the importance of three elements, described as follows. (1) Charge of the active site in the apo enzyme: apo-MDH had a positively charged pocket in the active site, whereas the active

[1]Division of Life Science, Graduate School of Science and Engineering, Setsunan University, 17-8 Ikeda-Nakamachi, Neyagawa, Osaka 572-8508, Japan.
[2]Department of Life Science, Setsunan University, 17-8 Ikeda-Nakamachi, Neyagawa, Osaka 572-8508, Japan.
Tel: +81-72-800-1151
Fax: +81-72-838-6599
E-mail: nishiya@lif.setsunan.ac.jp

*Corresponding author: Yoshiaki Nishiya, Department of Life Science, Setsunan University, 17-8 Ikeda-Nakamachi, Neyagawa, Osaka 572-8508, Japan.

Received for Publication: May 7, 2025
Accepted for Publication: June 11, 2025

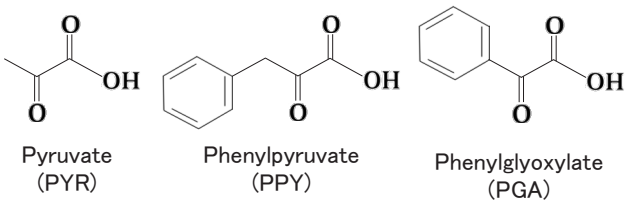

Fig. 1. Substrate structures of gs-LDH.

site of apo-LDH had almost no charge bias. (2) Movement of the catalytic histidine residue: the catalytic residue of MDH switched to an active location with the change from the open form to the closed form. However, the catalytic residue of LDH always showed an active location, regardless of the structural changes. (3) Flexibility of the mobile loop in the active site during structural changes: the mobile loop in MDH was less flexible than that in LDH and was difficult to spontaneously convert from the open form to the closed form.

Based on (1), the active site of MDH has a high affinity for oxaloacetate, which has a strong negative charge. In addition, the binding of oxaloacetate neutralizes the positive charge and reduces repulsion, promoting the transition to a closed conformation. Because of (2), the conversion of MDH to its closed form and the initiation of the reaction are linked, making the substrate specificity strict. In contrast, LDH does not have a switching mechanism; therefore, even its open form can react with certain substrates. Based on (3), the interaction between the mobile loop and the substrate is important for the conversion of MDH to the closed form, and oxaloacetate, which exhibits a strong interaction, is advantageous for closing the loop. In addition, the compact substrate-binding spaces in the closed forms of both enzymes are important for substrate selection in general enzyme–substrate complexes.

The combined effect of these three elements provides a strategy for MDH to achieve high substrate specificity. However, the simple reaction mechanism of LDH reduces its substrate selectivity[6,7]. Thus, LDH is a desirable basis for the functional alteration of substrate specificity[8-12]. A structural understanding of substrate specificities provides a theoretical basis for the structure-based computational design toward the development of diagnostic enzymes[13].

In this study, LDH from *Geobacillus stearothermophilus* (gs-LDH)[8] was used as the basic structure for site-directed mutagenesis, and a phenylpyruvate (PPY)-specific dehydrogenase was developed using structure-based enzyme design. PPY is one of the minor substrates for LDH and is structurally similar to the major substrate, pyruvate (PYR) (Fig. 1)[10].

PPY is neurotoxic and is rarely present in healthy living organisms. In phenylketonuria (PKU), large amounts of PPY are excreted in the urine along with phenylalanine because of impaired phenylalanine hydroxylation[14]. This metabolic product in excess inhibits normal metabolism, causing clinical symptoms such as mental retardation in newborns and infants. PPY has also been suggested to cause various psychiatric symptoms in adults in addition to oxidative stress. PKU is diagnosed by quantifying blood phenylalanine levels[15], and PPY is currently not measured.

We believe that this simple and rapid enzymatic measurement of PPY will be clinically significant. A PPY endpoint assay reagent containing the developed enzyme was prepared, and its practicality was preliminarily confirmed.

2. Materials and Methods

Reagents and chemicals

All the reagents and chemicals were purchased from Nacalai Tesque, Inc. (Kyoto, Japan) and Wako Pure Chemical Industries, Ltd. (Osaka, Japan).

Computational analysis

Based on the gs-LDH tertiary structure (PDB ID: 1LDN)[16], *in silico* analysis and rational mutation design were performed using the Molecular Operating

Table 1 Specific PCR primers used for site-directed mutagenesis

Q102A	Forward	5′-GCGAAACCGGGTGAAACCCGTCTGGACCTGGTGG-3′
	Reverse	5′-GTTCGCACCCGCGCAAATCACAACCAGATCCGCG-3′
A239G	Forward	5′-GGCTATCAAATCATTGAGAAGAAAGGTGCGACC-3′
	Reverse	5′-CGCATCACGCACGTTAACAAAGATACGTTCCAGG-3
I243A	Forward	5′-GGAGAAGAAAGGTGCGACCTACTATGGTATTGCG-3′
	Reverse	5′-GCGATTTGATACGCCGCATCACGCACGTTA-3′
T249A	Forward	5′-GTGCGGCGTACTATGGTATTGCGATG-3′
	Reverse	5′-CATAGTACGCCGCACCTTTCTTCTCAAT-3′

Underlines indicate mutation sites.

Environment software (MOE, Chemical Computing Group Inc., Montreal, Canada)[17,18]. Before energy minimization, the force field Amber10:EHT was used to add hydrogen atoms and partial charges according to the manufacturer's instructions. Relaxation of the added hydrogen atoms via energy minimization was performed using a conjugated gradient/truncated Newton optimization algorithm with a convergence criteria of 0.05 kcal/mol. Complex structural models of the wild-type (WT) and mutant enzymes containing PPY or PYR were constructed by docking simulations according to the manufacturer's instructions. The molecular structures of the compounds used in the docking simulations were obtained from the PubChem database (https://pubchem.ncbi.nlm.nih.gov/). Enzyme structure models were visualized using MOE software.

Site-directed mutagenesis

Expression plasmid cloning of gs-LDH (951 bp and 317 amino acid residues, accession number: LC100138 and WP_033016716, respectively) into the *NdeI* and *Bam*HI sites of pET-28a(+) (5,369 bp, Km^r) (GenScript, Inc., Piscataway, NJ, USA) was performed to prepare the WT and as a template for site-directed mutagenesis. The plasmid encodes gs-LDH and 20 extra amino-terminal residues containing a 6-histidine tag. Expression plasmids for the mutants were prepared by an inverse polymerase chain reaction (PCR) method using the enzyme solution of KOD-plus (Toyobo Co., Ltd., Osaka, Japan) or PrimeSTAR Max DNA Polymerase (Takara Bio Inc., Shiga, Japan) according to the manufacturer's instructions. The sequences of the PCR primers used are listed in Table 1.

Enzyme expression and purification

Each expression plasmid was transformed into *Escherichia coli* BL21(DE3). Recombinant cells were cultured in Luria–Bertani (LB) medium with 30 μg/mL kanamycin at 37°C and a shaker speed of 200 r/min for 1 h. Expression of the recombinant protein was induced by adding 100 μmol/L isopropyl β-D-1-thiogalactopyranoside to the LB medium at 37°C for 19 h. The cells were collected by centrifugation at 4°C and 13,000 ×g for 5 min and suspended in buffer A (20 mmol/L potassium phosphate, pH 7.5). After sonication on ice, the cell extracts were centrifuged at 13,000 ×g for 30 min to collect the supernatants. The protein solution was applied to a His GraviTrap™ Ni-chelating affinity chromatography column (Cytiva, Uppsala, Sweden) equilibrated with buffer A containing 500 mmol/L NaCl and 20 mmol/L imidazole. Bound protein was eluted stepwise using buffer A containing 500 mmol/L NaCl and 100–500 mmol/L imidazole. The protein solution was dialyzed against buffer A to remove the NaCl and imidazole.

Finally, each enzyme was purified to achieve homogeneity. The molecular weight was determined by sodium dodecyl sulfate-polyacrylamide gel electrophoresis (SDS-PAGE), and protein concentration was quantified using the Bradford assay (Takara Bio Inc.).

Dehydrogenase activity assay

The LDH reaction is reversible, and substrate

Table 2 Specific activities of WT and mutants

Enzyme	Specific Activity (U/mg)			PPY/PYR (%)	PPY/PGA (%)
	PYR	PPY	PGA		
WT	561	236	0.0885	42.1	2.67×10^5
Q102A	214	334	0.773	156	4.32×10^4
A239G	679	651	0.0549	95.8	1.18×10^6
I243A	532	75.6	0.432	14.2	1.75×10^4
Q102A+A239G	395	691	0.890	175	7.76×10^4
Q102A+A239G+T249A	6.58	271	0.0869	4110	3.12×10^5

reduction proceeds simultaneously with the oxidation of the coenzyme NADH. The PYR, PPY, and phenylglyoxylate (PGA, Fig. 1) dehydrogenase activities of each enzyme were monitored based on the decrease in NADH concentration, and the time-dependent spectral change at 340 nm was measured against a blank to quantify the NADH consumed using the molar extinction coefficient (6300 $M^{-1}\cdot cm^{-1}$). The enzyme solution (0.05 mL) was added to the assay solution (1.0 mL) containing 0.1 mol/L potassium phosphate buffer (pH 6.0), 10 mmol/L substrate, 10 mmol/L D-fructose-1,6-bisphosphate, and 0.2 mmol/L NADH. One unit (1 U) of activity was defined as the amount of enzyme that reduces 1 μmol of NADH per minute at 30°C.

According to the Michaelis–Menten equation, the kinetic parameters of the WT and mutants were determined based on their enzymatic activities at various substrate concentrations (0.5–8 mmol/L) at 30°C. All data were averaged over three independent experiments.

PPY assay

The decrease in NADH absorbance at 340 nm was measured using a spectrophotometer (U-3900; HITACHI, Tokyo, Japan). The working solution (WS) contained 0.1 mol/L potassium phosphate buffer (pH 6.0), 1 U/mL mutant enzyme, 10 mmol/L D-fructose-1,6-bisphosphate, and 0.2 mmol/L NADH. Next, 900 μL of WS was preheated at 30°C for 2 min, and 30 μL of PPY (0–1.2 mmol/L) was added. The changes in absorbance at 340 nm were measured in real time at 30°C for 5 min. Dilution linearity was calculated from the absorbance at 5 min. All data were averaged over three independent experiments.

3. Results and Discussion

Mutation design of gs-LDH to achieve high PPY affinity (1)

The dehydrogenase activity of gs-LDH toward PPY was approximately 42% of that toward PYR (Table 2). Because PPY is much bulkier than PYR (Fig. 1), an *in silico* mutation design for expanding the substrate-binding site of gs-LDH was attempted to develop a PPY-specific dehydrogenase.

The gs-LDH–PPY complex structure was constructed by docking simulation, and mutants with a lower docking score (S value) than that of the WT were searched. The S value represents the energetic stability of enzyme–substrate interactions; therefore, smaller values indicate more stable interactions, that is, higher affinities. The S value for the WT-PPY complex was −6.4, whereas those for Q102A-PPY, A239G-PPY, and I243A-PPY complexes were −7.3, −6.6, and −6.7, respectively (Fig. 2). Three mutants were predicted to be more energetically stable in binding with PPY than the WT and were selected as candidates for improving PPY specificity.

PPY dehydrogenase activity of mutants

The expression plasmids for the Q102A, A239G, and I243A mutants were created by site-directed mutagenesis. Subsequently, the WT and mutant gs-LDHs were purified to homogeneity from the recombinant *E. coli* strains, as described in the Materials and Methods. The molecular weights of all the enzymes were estimated to be approximately 37 kDa

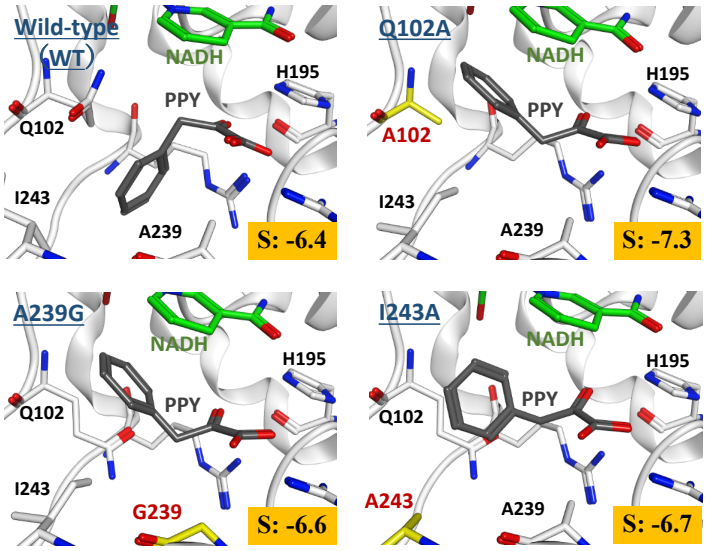

Fig. 2. Predicted complex structures of wild-type (WT) and mutant PPY. The main chain is represented by a ribbon model. The side chains, coenzyme NADH, and substrate PPY are represented using a stick model. The mutated residues, NADH, PPY, oxygen, and nitrogen atoms are shown in yellow, green, gray, red, and blue, respectively. The S value in each lower-right corner is the docking score, which indicates the energy stability of a complex structure.

by SDS-PAGE, corresponding to the amino acid sequences (data not shown).

The enzymatic activities of the mutants were measured and compared with those of the WT (Table 2). The specific activities of Q102A and A239G against PPY were approximately 1.4- and 2.8-fold higher, respectively, than those of WT. The PPY/PYR-specific activity ratios for Q102A and A239G were 156% and 95.8%, respectively, compared with 42.1% for the WT. Thus, the specificity of both mutants for PPY improved. However, the specific activity of I243A against PPY was decreased. Docking simulations suggested that gs-LDH interacted with the benzene ring of PPY at position 243 (Fig. 2). The reduced PPY dehydrogenase activity of I243A most likely decreased its hydrophobic interaction with the benzene ring of PPY owing to the I-to-A mutation.

The specific activities of the WT and mutants, which are structurally similar to those of PPY, against PGA (Fig. 1), were also measured (Table 2). Although mutational effects were observed, these activities were much lower than those of PYR and PPY. This result could be due to the lower structural flexibility of PGA. In fact, the conformational comparison of PPY and PGA using the low-mode molecular dynamics analysis of the MOE software demonstrated that PGA had much fewer possible structures than PPY did (data not shown).

The gene encoding the double mutant Q102A+A239G was also generated, and the enzyme was purified to homogeneity. As shown in Table 2, the double mutant exhibited an additive effect of Q102A and A239G. The specific activity of Q102A+A239G against PPY was 691 U/mg, and the PPY/PYR specific activity ratio was 175%, resulting in an improvement over single mutations. However, the PYR dehydrogenase activity of Q102A+A239G was still high, at approximately 70% of that of the WT. Further improvement of PPY specificity is desirable for its use as an analytical enzyme.

Mutation design of gs-LDH to achieve high PPY affinity (2)

Additional mutations to combine with the double mutant were investigated to improve PPY specificity. Consequently, the T-to-A mutation at position 249 expanded the substrate pocket by replacing it with a smaller side chain. When the tertiary structure model of the triple mutant Q102A+A239G+T249A was constructed and compared with that of the double mutant, spatial expansion around the catalytic residue H195 was confirmed, as expected (Fig. 3). Therefore,

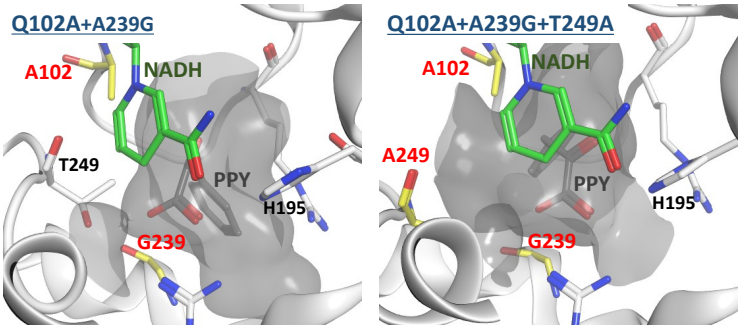

Fig. 3. Predicted complex structures of Q102A+A239G and Q102A+A239G+T249A with PPY. The main chain is represented by a ribbon model. The side chains, coenzyme NADH, and substrate PPY are represented using a stick model. The mutated residues, NADH, PPY, oxygen, and nitrogen atoms are shown in yellow, green, gray, red, and blue, respectively. The substrate-binding pockets are indicated by transparent gray areas.

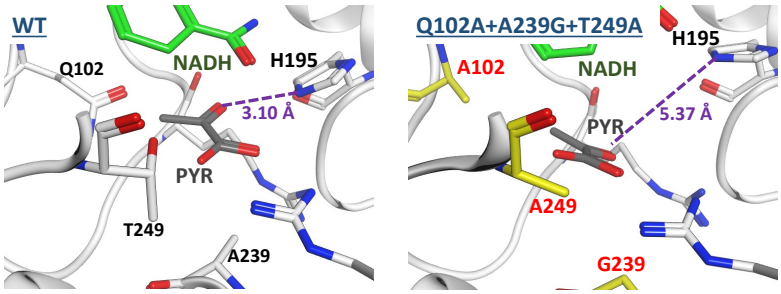

Fig. 4. Predicted complex structures of WT and Q102A+A239G+T249A with PYR. The main chain is represented by a ribbon model. The side chains, coenzyme NADH, and substrate PYR are represented using a stick model. The mutated residues, NADH, PYR, oxygen, and nitrogen atoms are shown in yellow, green, gray, red, and blue, respectively. The distances between the catalytic residues H195 and PYR are indicated in purple.

T249A was selected as a candidate gene to further improve PPY specificity.

Properties of the triple mutant

The triple mutant Q102A+A239G+T249A was purified to homogeneity, and its enzymatic activities were compared with those of the WT and other mutant gs-LDHs (Table 2). Among the mutants generated in this study, Q102A + A239G + T249A exhibited the highest PPY specificity. The PYR dehydrogenase activity and PPY/PYR specific activity ratios were approximately 1.1% and 4100% (98-fold) of those of the WT. Therefore, we developed a PPY-specific dehydrogenase.

Decreased PYR dehydrogenase activity in Q102A +A239G+T249A cells was explained by *in silico* structural analysis (Fig. 4). In the WT structure, the distance between the catalytic residue H195 and PYR was appropriate at 3.10 Å, whereas the distance was 5.37 Å in the Q102A+A239G+T249A structure model. The longer distance in the triple mutant may reduce the proton transfer efficiency of H195 to PYR and decrease its activity against PYR.

The PPY reaction curves of the WT and Q102A+ A239G+T249A are shown in Fig. 5. The K_m values of WT and Q102A+A239G+T249A ($V_{max}/2$ value for WT due to the sigmoid reaction curve) were estimated to be 1.6 and 0.35 mmol/L, respectively. High PPY affinity for Q102A+A239G+T249A was demonstrated.

PPY assay using the triple mutant

The endpoint assay reagent containing the PPY-specific triple mutant was prepared and utilized

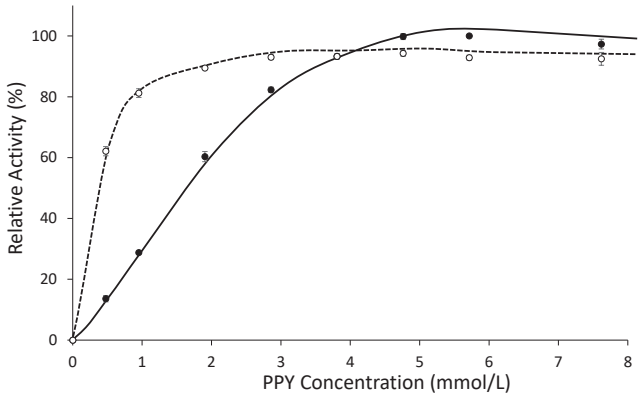

Fig. 5. Substrate (PPY)–activity curves of WT and Q102A+A239G+T249A mutants. Solid lines with closed circles and dotted lines with open circles indicate WT and Q102A+A239G+T249A mutants, respectively. Error bars represent the standard deviation (n = 3).

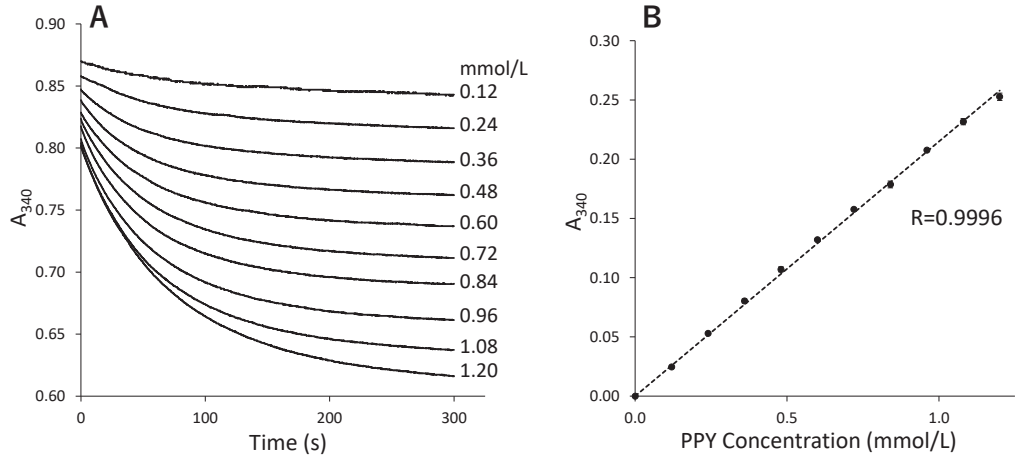

Fig. 6. PPY assays using Q102A+A239G+T249A. A: Reaction time course. The concentration of each PPY is shown in the graph. B: Linearity. Error bars represent the standard deviation (n = 3). R values represent the correlation coefficients.

in the PPY assay as described in the Materials and Methods section. The time courses of PPY measurement were observed, showing that end points were nearly attained within 5 min at all concentrations (0.12–1.20 mmol/L) (Fig. 6A). In addition, the high linearity of the PPY concentration was estimated at a correlation coefficient of 0.9996 (Fig. 6B). These results suggest that the triple mutant can be used for endpoint assays of PPY within the range measured in this study. Its application to actual samples is important for future practical use.

Conflicts of interest

The authors declare no conflict of interest.

Acknowledgements

We thank Shotaro Yamaguchi for technical support. We are grateful to Dr. Yuya Shimozawa for helpful discussion. We would like to thank Editage (www.editage.jp) for the English language editing.

References

1. Shimozawa Y and Nishiya Y: Malate dehydrogenase of *Geobacillus stearothermophilus:* A practically feasible enzyme for clinical and food analysis. Int J Anal Bio-Sci, 7:59-67, 2019.
2. Shimozawa Y, Himiyama T, Nakamura T, and Nishiya

Y: Structural analysis and reaction mechanism of malate dehydrogenase from *Geobacillus stearothermophilus*. J Biochem, 170:97-105, 2021.

3. Shimozawa Y, Himiyama T, Nakamura T, and Nishiya Y: Increasing loop flexibility affords low-temperature adaptation of a moderate thermophilic malate dehydrogenase from *Geobacillus stearothermophilus*. Protein Eng Des Sel, 34:gzab026, 2021.
4. Shimozawa Y, Himiyama T, Nakamura T, and Nishiya Y: Structural analysis of diagnostic enzymes: Differences in substrate specificity between malate dehydrogenase and lactate dehydrogenase [Jpn]. J Anal Bio-Sci, 44:151-159, 2021.
5. Shimozawa Y, Mtsuhisa H, Nakamura T, Himiyama T, and Nishiya Y: Reducing substrate inhibition of malate dehydrogenase from *Geobacillus stearothermophilus* by C-terminal truncation. Protein Eng Des Sel, 35:gzac008, 2022.
6. Davies DD and Davies S: Purification and properties of L(+)-lactate dehydrogenase from potato tubers. Biochem J, 129:831–839, 1972.
7. Steinbüchel A and Schlegel HG: NAD-linked L(+)-lactate dehydrogenase from the strict aerobe *Alcaligenes eutrophus*. Eur J Biochem, 130:321-328, 1983.
8. Wilks HM, Hart KW, Feeney R, Dunn CR, Muirhead H, Chia WN, Barstow DA, Atkinson T, Clarke AR, and Holbrook JJ: A specific, highly active malate dehydrogenase by redesign of a lactate dehydrogenase framework. Science, 242:1541-1544, 1988.
9. Binay B, Sessions RB, and Karagüler NG: A double mutant of highly purified *Geobacillus stearothermophilus* lactate dehydrogenase recognises L-mandelic acid as a substrate. Enzyme Microbial Technol, 52:393-399, 2013.
10. Li JF, Li XQ, Liu Y, Yuan FJ, Zhang T, Wu MC, and Zhang JR: Directed modification of L-LcLDH1, an L-lactate dehydrogenase from *Lactobacillus casei*, to improve its specific activity and catalytic efficiency towards phenylpyruvic acid. J Biotechnol, 281:193-198, 2018.
11. Wu B, Yu Q, Zheng S, Pedroso MM, Guddat LW, He B, and Schenk G: Relative catalytic efficiencies and transcript levels of three D- and two L-lactate dehydrogenases for optically pure D-lactate production in *Sporolactobacillus inulinus*. Microbiologyopen, 8, 2019.
12. Wu A, Bai Y, Fan TP, Zheng X, and Cai Y: Modified catalytic performance of *Lactobacillus fermentum* L-lactate dehydrogenase by rational design. Systems Microbiol Biomanufact, 2:473-486, 2022.
13. Hiruta M and Nishiya Y: Creation of an L-mandelate oxidase via structure-guided design of engineered lactate oxidase. Int J Anal Bio-Sci, 6:25-29, 2018.
14. Spronsen FJ, Blau N, Harding C, Burlina A, Longo N, and Bosch AM: Phenylketonuria. Nature Rev Disease Primers, 7:No.36, 2021.
15. Wendel U, Hummel W, and Langenbeck U: Monitoring of phenylketonuria: A colorimetric method for the determination of plasma phenylalanine using L-phenylalanine dehydrogenase. Anal Biochem, 180:91-94, 1989.
16. Wigley DB, Gamblin SJ, Turkenburg JP, Dodson EJ, Piontek K, Muirhead H, and Holbrook JJ: Structure of a ternary complex of an allosteric lactate dehydrogenase from *Bacillus stearothermophilus* at 2.5 Å resolution. J Mol Biol, 223:317-335, 1992.
17. Nishiya Y, Toyama F, and Zhang Y: Computational insights for coenzyme interactions in wild-type and mutant sarcosine oxidases. Int J Anal Bio-Sci, 11:111-116, 2023.
18. Nishiya Y, Ishihara H, Zhang Y, and Toyama F: Rational alteration of the pH profile of sarcosine oxidase by site-directed mutagenesis around the active site. Int J Anal Bio-Sci, 12:15-20, 2024